ScieRxiv
NOT PEER-REVIEWED
Original Article

Diagnostic potential of circulating miRNAs for early and non-invasive detection of lipedema

Eleni Priglinger[1,2,3*], Karin Missfeldt[1,2,3], Marianne Pultar[4], Martin Barsch[5], Matthias Sandhofer[6], Sandra Milić[2,3], Viktoria Sperrer[1,3], Johannes Österreicher[2,3], Wolfgang Holnthoner[2,3], Silvio Kau-Strebinger[7], Matthias Hackl[4], Susanne Wolbank[2,3*]

[1]Johannes Kepler University Linz, Kepler University Hospital, Department for Orthopaedics and Traumatology, 4020 Linz, Austria.

[2]Ludwig Boltzmann Institute for Traumatology, AUVA Research Center, 1200 Vienna, Austria.

[3]Austrian Cluster for Tissue Regeneration, 1200 Vienna, Austria.

[4]TAmiRNA, 1110 Vienna, Austria.

[5]Center for Lipedema, 4020 Linz, Austria.

[6]Center for Lipedema, Diagnosis and Therapy, 1010 Vienna, Austria.

[7]Department of Biological Sciences and Pathobiology, Unit of Morphology, University of Veterinary Medicine, 1210 Vienna, Austria.

***Correspondence to: Dr.** Eleni Priglinger, Johannes Kepler University Linz, Kepler University Hospital, Department for Orthopaedics and Traumatology, 4020 Linz, Austria. E-mail: eleni.priglinger@jku.at; Dr. Susanne Wolbank, Ludwig Boltzmann Institute for Traumatology, AUVA Research Center, 1200 Vienna, Austria. E-mail: susanne.wolbank@trauma.lbg.ac.at

Received: 08 May 2026 | Approved: 20 May 2026 | Online: 20 May 2026

Abstract

Aim: Lipedema is a painful chronic condition characterized by progressive enlargement of adipose tissue in the extremities, frequently misdiagnosed as obesity due to a lack of objective measures. This study investigated circulating miRNAs in peripheral blood plasma and plasma sEVs as potential diagnostic biomarkers for lipedema.

Methods: Plasma and plasma-sEV miRNA levels were investigated by untargeted small RNA sequencing in: lipedema (BMI < 30) and lipedema/obesity (BMI > 30) *vs.* control individuals with (BMI > 30) or without obesity (BMI < 30). MiRNAs were selected for validation by RT-qPCR and logistic regression analysis was applied to evaluate the diagnostic performance of candidate miRNAs. In silico target prediction analysis was performed to explore biological relevance

.

Results: The largest effects were observed at BMI > 30 comparing lipedema *vs.* control plasma, with 70 downregulated and 10 upregulated miRNAs. In sEVs one miRNA was upregulated in lipedema *vs.* control (BMI < 30), and one up- and five downregulated comparing lipedema/vs control (BMI > 30). 29 miRNAs were cross-validated by RT-qPCR and validated in 16 additional samples. Five circulating miRNAs (miR-223-3p, miR-224-5p, miR-3651, miR-484, miR-92b-3p) were confirmed to distinguish lipedema from control individuals independent from BMI. Multiple logistic regression analysis showed that miR-224-5p and miR-3651 correctly classified nearly 80% of lipedema and control individuals, achieving 75% sensitivity and 92% specificity. MiRNA target prediction combined with pathway analyses indicate involvement in systemic pathophysiological processes relevant to lipedema.

Conclusion: Circulating miRNAs discriminated lipedema from control individuals across different BMIs, hence representing promising diagnostic biomarkers. The identified miRNA signature provides insights into lipedema pathophysiology on a systemic level.

Keywords: Lipedema, obesity, diagnosis, biomarkers, micro-RNAs (miRNAs), extracellular vesicles

INTRODUCTION

Lipedema is a chronic progressive condition characterized by disproportionate deposition of subcutaneous adipose tissue, predominantly in the extremities. Clinically, lipedema presents pain, swelling, and increased sensitivity in the affected areas, which often leads to progressive functional limitations and psychological distress[1]. Lipedema patients represent approximately 12% in the female population[2]. but are still largely under- or misdiagnosed as obesity or lymphedema, delaying or preventing appropriate treatment. Liposuction performed under high volume tumescent anesthesia is currently the only effective treatment for reducing the disproportionate fat deposits[3]. The etiology of lipedema remains poorly understood, but likely involves a combination of genetic, hormonal, and inflammatory factors[4,5]. Since the onset of the disease is driven during hormonal changes, estrogen signaling has been investigated as one key regulator[6,7]. Lipedema is characterized by both adipocyte hypertrophy and hyperplasia, impaired stem cell differentiation and apoptosis[8,9]. Chronic inflammation, aberrant angiogenesis and remodeling of blood and lymphatic vessels contribute to disease progression, even at its early stages[10,11].

Despite its high prevalence, the lack of reliable diagnostics hinders early and accurate diagnosis, highlighting the urgent need for objective molecular biomarkers.[4] Current diagnostic approaches rely on clinical anamnesis, physical inspection, and ultrasound. These methods often lack specificity and are insufficient for distinguishing lipedema from related conditions[12]. Recent advancements have identified potential biomarkers such as tissue sodium content[13], cytokine profile and biochemical composition involved in lipid metabolism[14]. Novel imaging modalities for adipose tissue include 3D-visualization of human blood vasculature using ESAM antibody[15]. At systemic level, changes in metabolites have been investigated, especially pyruvic acid[16], adipokines and vitamin D[17]. Notably, elevated Platelet Factor 4 (PF4) has been identified as a potential biomarker for lymphatic vasculature dysfunction[18].

MicroRNAs (miRNAs) are short non-coding RNAs regulating gene expression by targeting messenger RNAs (mRNAs), leading to their degradation or inhibition of translation[19]. Found in bio-fluids such as plasma, miRNAs are circulating associated

to extracellular vesicles (EVs) or bound to protein complexes[20]. The biomolecular cargo of EVs reflects the (patho)physiological state of their cells of origin, making them valuable candidates for diagnostic and prognostic biomarkers[21]. Studies in other adipose-related conditions, such as obesity and metabolic syndrome, have identified miRNAs associated with adipocyte differentiation (e.g., miR-130, miR-143), inflammatory signaling (e.g., miR-155, miR-21), and vascular homeostasis (e.g., miR-126, miR-92a), suggesting a potential role for these molecules in lipedema[22]. We have previously characterized in early-stage lipedema patients total and small EV (sEV)-contained miRNAs in the secretome of the stromal vascular fraction (SVF) of adipose tissue[3,9]. We identified one non-sEV and seven sEV-associated regulated miRNAs that are mediators of processes, such as Wnt and TGF-β signaling, that may contribute to disease progression[10].

This study investigates circulating miRNAs as blood-based biomarkers for lipedema and explores their reflection of pathophysiology. Using an unbiased small RNA-sequencing approach, we analyzed both total plasma and sEV-contained miRNA fractions in lipedema versus BMI-matched controls.

METHODS

Patient cohorts

Ethical approval (1339/2021) from the local JKU ethical board, and all procedures were conducted in accordance with the Declaration of Helsinki. Written informed consent was obtained from all participants. Lipedema was defined by clinical anamnesis (disproportional fat accumulation at knees/ankles with spared forefoot/toes), impedance measurement and ultrasound to exclude phlebedema, varicose veins, and lymphedema. Structural changes were documented. Patients were classified per S1 guidelines and grouped into: “lipedema” stage 1-2, type I+II, BMI < 30 and “lipedema obese” stage 2-4, type I-IV, BMI >30. Controls included a “non-obese control” cohort (BMI < 30) and a cohort with a BMI >30 based on impedance, without metabolic syndrome, and clinical fat distribution, designated “obese control”. Participants were self-identified as European/Caucasian, aged 25-45 years Only women were included, as lipedema predominantly affects women. Exclusion criteria were high-intensity sports, endometriosis, PCO-syndrome, thrombophilia, Leiden mutation, and neurological

disorders.

Sample preparation

Peripheral blood was processed to obtain platelet-poor plasma (PPP) following *Mussbacher et al*[23]. Blood was drawn at least 8 h following the last meal using a 10 mL K_2EDTA plasma tube (BD Vacutainer 366643), mixed by inverting and placed on ice. 90-120 min later, tubes were centrifuged in a fixed-angle rotor (ThermoFisher Heraeus Multifuge X3R) at 1,000 g for 10 min at 4 °C. Plasma was carefully removed, hemolysis state was assessed measuring optical density (OD) at 414 nm on a plate reader (Tecan infinite M200 Pro, Tecan Group, Switzerland). Tubes were further centrifuged at 10,000 g for 10 min at 4 °C and. aliquots stored at -80 °C within 30 min after centrifugation. Hemolysis was assessed measuring optical density (OD) at 414 (Tecan infinite M200 Pro). sEVs (< 200 nm) were enriched by Amicon 30 kDa MWCO ultrafiltration (Merck, Darmstadt, Germany) and separated from protein fractions using size exclusion chromatography (qEVsingle columns 15928090, Izon, New Zealand). In brief, 150 µL of PPP were loaded onto the column, followed by 2.5 mL DPBS. A void volume of 870 µL was discarded before collection of 670 µL as sEV-fraction.

EV characterization

(Fluorescent) Nanoparticle tracking analysis (NTA/f-NTA)

For sEV quality assurance, samples were characterized on a ZetaView x30 QUATT (Particle Metrix, Germany). Hydrodynamic particle diameter and concentration were measured at 25 °C in scatter mode (488 laser). Instrument settings were: Sensitivity 80, shutter speed 100, minimum brightness threshold 20, maximum brightness 255, minimum area10 pixels, maximum area 1000 pixels, gain 28.8, frame rate 30 and trace length 15. Quality control followed manufacturer's recommendations of 100-400 particles/frame and > 500 total traced particles per measurement. Bilipid membrane enclosed particles were assessed by CellMask™ Green (CMG; Thermo Fisher, USA) following Oesterreicher *et al.*[24]. Data were acquired using ZetaView software version 8.05.12 SP2 (Particle Metrix).

Transmission electron microscopy (TEM)

EVs from one obese donor (29) were characterized using TEM following our previous

protocol[25]. EVs were adsorbed onto formvar/carbon-coated nickel grids, blocked with 0.2% BSA in freshly filtered PBS (w/o Ca^{++}/ Mg^{++}), and labeled with mouse anti-human CD81 (clone JS-81; BD Biosciences, USA), followed by 10 nm colloidal gold-conjugated goat anti-mouse (Sigma-Aldrich, USA). A no sample and no primary antibody control was performed. After fixation and uranyl acetate staining, grids were imaged using a Zeiss EM 900 TEM (Carl Zeiss Microscopy, Germany, electron-sensitive digital Frame-Transfer-CCD camera and ImageSP software (Tröndle, Germany with SYSPROG, Belarus)). For size determination, ImageJ software version 2.9.0/1.53t (NIH, USA) was used.

MiRNA analyses

Total RNA isolation

RNA was extracted from 200 µL plasma and sEVs using the miRNeasy Mini Kit (Qiagen, Germany), with the following modifications: miRCURY spike-in mix (Qiagen) was added to Qiazol before sample lysis, and 7 µL glycogen (5 mg/mL) were added to 650 µL aqueous phase following chloroform extraction for precipitation efficiency. Total RNA was eluted in 30 µL nuclease-free water and stored at -80 °C until further analysis.

Small RNA library preparation

The miRNA Next-Generation-Sequencing (NGS) Discovery Assay (miND®, TAmiRNA, Austria) was used for untargeted analysis of short non-coding RNAs in plasma and sEV samples. 8.5 µL RNA was used as input for the generation of small RNA sequencing libraries using the RealSeq Biofluids library preparation kit (RealSeq Biosciences, USA) according to the manufacturer's instructions. To each sample, 1 µL miND® spike-in standards (TAmiRNA) were added during the first step as described previously[26]. Adapter-ligated libraries were PCR-amplified using barcoded Illumina reverse primers in combination with the Illumina forward primer. Library quality control was performed using Fragment Analyzer NGS fragment kit (Agilent Technologies). All samples were pooled equimolarly and processed with the Blue Pippin system (Sage Science, USA) using 3% agarose size selection cassettes, following the manufacturer's instructions (size range: 130-160 bp). Sequencing was performed on a NextSeq 2,000 system (Illumina) with 100-bp single-end reads.

Small RNA-sequencing data analysis

NGS data was analyzed using the miND® analysis pipeline[27] and evaluated with fastQC v0.11.9 and multiQC v1.14. Reads were adapter-trimmed and quality filtered using cutadapt v3.3. Mapping steps were performed with Bowtie v1.3.0 and miRDeep2 v2.0.1.2. Reads were initially mapped against the human genomic reference GRCh38.p12 by Ensembl allowing two mismatches and subsequently against miRBase v22.1, filtered for miRNAs of homo sapiens (hsa), allowing one mismatch. For a general RNA composition, non-miRNA mapped reads were mapped against RNAcentral v19.0 and assigned to RNA species of interest. Additional NGS quality control and absolute quantification of miRNAs was done using miND® spike-ins based on a linear regression model. Read counts were normalized per million miRNA reads and further used for unsupervised analyses to evaluate data variability, followed by differential expression analysis based on generalized linear models to identify significantly regulated miRNAs as implemented in EdgeR (R, Bioconductor) including Benjamini-Hochberg adjustment of *p*-values for multiple testing.

RT-qPCR analysis

Starting from total RNA samples, cDNA was synthesized using the miRCURY RT Kit (Qiagen, Germany). Reaction conditions were set according to recommendations by the manufacturer and 2 µL total RNA used as input in a 10 µL reaction. Quantitative PCR reactions were set up using miRCURY SYBR® green master mix with a 1:50 diluted cDNA and commercial LNA-enhanced primer assay. Reactions were performed in 384-well primer spotted plates in a LC480 II instrument (Roche, Germany) with 95 °C for 10 min, 45 cycles of 95 °C for 10 s and 60 °C for 60 s, followed by melting curve analysis. The second derivative maximum method was used to calculate cycle of quantification values (Cq-values).

Target prediction and pathway analysis

Using the tool miRNAtap v1.38.0 we combined the results of 5 different miRNA-mRNA interaction databases (DIANA, Miranda, PicTar, TargetScan, and miRDB) to obtain a prediction of ranks for each target gene as well as the aggregated rank product. The number of target genes was filtered by specifying a minimum of 3

databases where the target gene must be found. Enriched GO terms biological processes (BP) were identified using topGO v2.56.0. Fisher test using all GO annotated human genes in org.Hs.eg.db v3.19.1 as reference was performed to calculate enrichment scores. BPs were summarized based on their similarities using rrvgo v1.16.0.

Statistical data analysis

Statistical analysis of normalized RT-qPCR data was performed in GraphPad Prism v10.5.0. Kruskal-Wallis tests with Dunn's multiple comparison analysis was used to compare non-normal distributed data between 3 or more groups. *P*-values were corrected for multiple testing using statistical hypothesis testing. Pearson correlation analysis was performed in R using complete observations and visualized using corplot function. Multiple logistic regression analysis was performed in R using the caret function. NTA data was screened for outliers using ROUT method at Q 1% and tested for normal distribution using D'Agostino/ Pearson test. Accordingly, parametric or non-parametric statistics were computed for group comparisons.

RESULTS

Cohorts and sample characterization

An overview of the study design is outlined in Figure 1. 40 study participants aged 25-45 were recruited and divided into four cohorts based on BMI and clinical diagnosis: non-obese (n = 16), lipedema (n = 12), obese (n = 6) and lipedema obese (n = 6). Age- and BMI-distribution across groups are summarized in Table 1. Cohort details, including sports activity, menstrual cycle status, smoking status, autoimmune disease and medication are summarized in Supplementary Table 1. Hemolytic status of plasma samples and BMI distribution across all cohorts are summarized in Supplementary Figures 1 and 2.

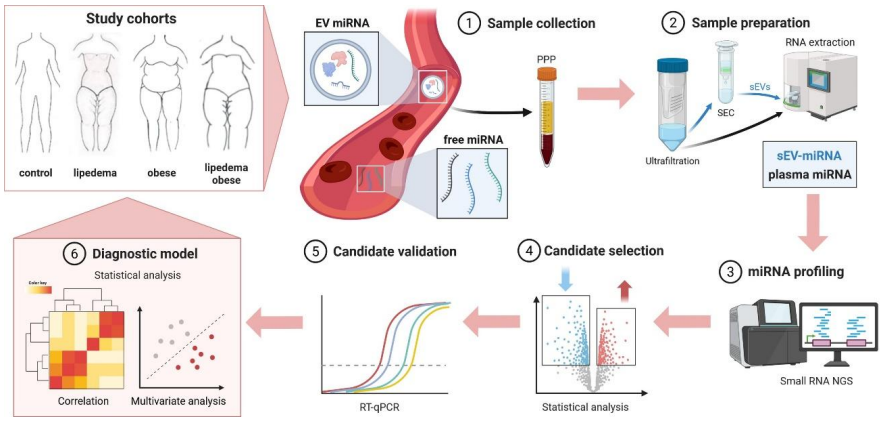

Figure 1. Study workflow for identifying miRNA biomarkers in lipedema. Study cohorts; (1) Sample collection: Peripheral blood was collected for study cohorts - non-obese controls (BMI < 30), lipedema (BMI < 30), obese controls (BMI > 30), and lipedema obese (BMI > 30 - followed by preparation of platelet-poor plasma (PPP); (2) Sample preparation: plasma was processed for RNA extraction, with small extracellular vesicles (sEVs) being separated using ultrafiltration and size-exclusion chromatography (SEC) to distinguish sEV-associated miRNAs (sEV-miRNA) from total circulating miRNAs (plasma miRNA); (3) miRNA profiling: Small RNA next-generation sequencing (NGS) was performed to identify differentially expressed miRNAs; (4) Candidate selection: Differential expression analysis was conducted to identify miRNA candidates that distinguish cohorts; (5) Candidate validation: Selected miRNAs were validated using quantitative real-time PCR (RT-qPCR) including an independent set of samples; (6) Diagnostic model: Correlation and multivariate statistical analyses were applied to evaluate the potential of miRNAs as biomarkers for lipedema diagnosis. Image created in https://BioRender.com.

Table 1. Cohort characteristics.

	Control		**Lipedema**		**Obese**		**Lipedema-obese**	
No	BMI (kg/m^2)	Age (years)	BMI (kg/m^2)	Age (years)	BMI (kg/m^2)	Age (years)	BMI (kg/m^2)	Age (years)
1	19.6	25	29.3	28	39.0	36	30.2	24
2	15.8	26	20.1	38	34.2	21	42.7	47
3	19.4	25	24.2	39	38.0	42	34.4	36
4	26.5	21	27.0	39	33.0	46	41.7	62

5	24.3	35	24.8	21	43.0	47	33.7	46
6	23.5	33	21.0	35	32.0	51	34.4	45
7	25.5	34	23.5	32	35.0	34	-	-
8	16.4	31	26.7	36	-	-	-	-
9	23.7	29	27.9	30	-	-	-	-
10	25.3	43	24.5	22	-	-	-	-
11	20.3	32	30.5	22	-	-	-	-
12	25.0	36	22.0	28	-	-	-	-
13	23.1	35	-	-	-	-	-	-
14	27.9	34	-	-	-	-	-	-
Mea	25.1	30.8	22.4	31.4	36.3	39.6	36.2	43.3
n	3.2	6.7	3.6	5.4	3.9	10.2	4.9	12.6
SD								

BMI and age of all study participants divided into four cohorts: control, lipedema, obese, and lipedema-obese. Abbreviations: BMI= body mass index. SD= standard deviation.

To evaluate the identity and structural integrity of nanoparticles enriched in plasma-sEV preparations, we employed NTA, TEM, and FT-FC. NTA of enriched particles revealed a modest yet significant increase in hydrodynamic diameter (median size and size distribution) in the obese and both lipedema groups compared to non-obese controls [Figure 2A]. TEM identification and sizing of EVs displayed negative staining contrast enhancement and accentuated cup-shaped morphology and a median particle diameter of 75 nm [Figure 2B] within the NTA measured size distribution range [Figure 2C]. Immunogold TEM for EV surface marker CD81 demonstrated specific labeling on a vesicle subset of vesicles, validating the presence of EVs in the preparations [Figure 2F].

An average > 90% of particles was CMG+, indicating presence of EVs. A significant reduction in the relative frequency of CMG+ particles was observed in preparations from all lipedema patients (BMI < 30 and BMI > 30), while EVs from individuals with obesity showed a similar trend [Figure 2D] compared to non-obese controls. Such changes may reflect alterations in EV membrane-associated components (biomolecular corona) that limit CMG incorporation but also could tune EV tropism. Compared to the

BMI < 30 cohorts, a slightly higher total number of particles was found in samples from individuals with obesity [Figure 2E].

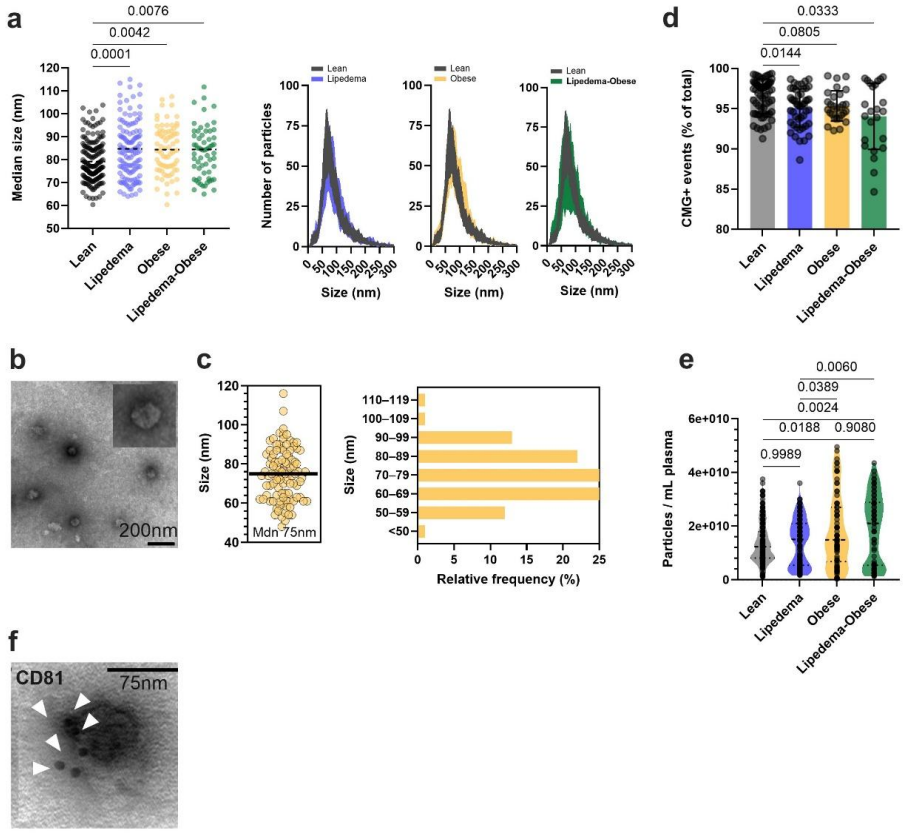

Figure 2. Orthogonal characterization of plasma-derived sEV preparations reveals disease-associated particle properties and confirms that lipid membrane-enclosed vesicles represent the predominant enriched particle fraction. (A) Median hydrodynamic particle diameter (X50, left) and size distribution profiles (right; 5nm size bins) measured by scatter NTA. Disease groups and obese controls show larger particle sizes compared to non-obese controls. *One-way ANOVA*, *Tukey's multiple comparisons*; X50 with n = 11 technical replicates * biological replicates (=donors) n = 16 non-obese controls, n = 12 lipedema, n = 7 obese controls, n = 6 lipedema-obese; (B) Representative TEM micrographs of sEVs separated from human plasma (donor 29); no primary antibody control. Overview image showing multiple contrast-enhanced particles attached to the grid surface and close-up image (insert) showing, albeit only accentuated, their cup-shaped structure; (C) TEM based sizing of particles attached to grids reveals size distribution like in NTA. 102 particles across 10 high-magnification fields manually sized; (D) Percentage of CMG lipophilic membrane dye positive events

relative to total events in fNTA. Data reveal an overall high proportion of membrane enclosed particles. Data shown as mean ± SD. *Kruskall-Wallis test*, *Dunn's multiple comparisons*; n = 4 technical replicates (independent measurements) per donor; (E) Particle concentration measurements using scatter NTA. Lipedema obese patients showed the highest total enriched particle numbers. *One-way ANOVA*, *Tukey's multiple comparisons*; n = 11 technical replicates per donor; (F) Representative immunogold TEM micrograph of sEVs separated from human plasma (donor 29). Arrowheads indicate bound 10nm colloidal gold particles to EV surface displayed CD81.

Small RNA-sequencing reveals marked differences between lipedema obese and obese cohort in total miRNA fraction

Small RNA-sequencing was used as untargeted analysis for a deep quantitative insight into circulating miRNAs including those packaged within sEVs. Samples from 24 participants representing all four cohorts showed homogeneous sequencing depth, with a median of 17-19 million reads. Recovery of miRNAs was similarly uniform, yielding 6 to 8 million reads, and consistent detection of 800 to > 1,000 miRNAs per sample [Supplementary Figure 3 A-C]. Likewise, sEV samples exhibited homogeneous total sequencing depth (13-18 million reads), and miRNA recovery was homogeneous but markedly lower (21,000-34,000 reads). Consequently, the number of detected miRNAs in plasma sEVs was also consistent across groups, but significantly lower compared to plasma, ranging from 250 to 360 [Supplementary Figure 3 D-F].

Next, we performed differential expression analysis to identify significantly altered miRNAs (FDR < 0.1) in plasma [Figure 3A] and plasma sEV [Figure 3B] samples, comparing lipedema patients to the respective control groups, stratified by low- and high-BMI. The analysis revealed marked differences between BMI groups. In plasma from obese lipedema patients versus obese controls, 80 miRNAs were differentially expressed - 10 upregulated and 70 downregulated [Figure 3C]. In contrast, plasma sEVs from the same comparison yielded only 6 differentially expressed miRNAs (miR-3960 upregulated, miR-26a-5p, miR-26b-5p, miR-142-3p, miR-423-3, miR-143-3p downregulated). When comparing lipedema with non-obese control, miR-125b-5p was upregulated in the sEV-fraction, while in plasma miR-133a-3p was upregulated. The low number of regulated miRNAs in sEVs may be a consequence of

the lower miRNA complexity in EVs and suggests that the plasma sEV-fraction may be less suitable for establishing robust miRNA-signatures of lipedema.

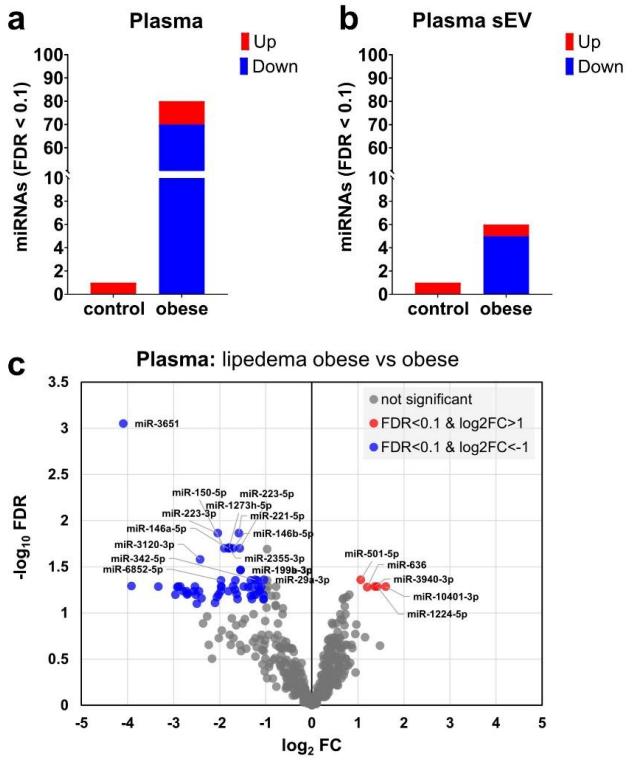

Figure 3. Small RNA next-generation sequencing analysis of miRNAs in lipedema patients versus control individuals. (A) Number of up- (red) and down-regulated (blue) miRNAs in plasma of lipedema patients compared to controls stratified by body mass index (BMI) = 30 into non-obese (control) or obese; (B) Number of up- (red) and down-regulated (blue) miRNAs in plasma sEVs of lipedema patients compared to controls stratified by BMI; (C) Volcano plot illustrating changes in plasma miRNA levels in lipedema obese patients versus obese controls. Analysis was stratified by BMI of 30. (n = 24).

Based on the differential expression results, we focused subsequent analyses on plasma miRNA profiles, specifically those identified between lipedema obese and obese controls. From this dataset, we selected 29 candidate miRNAs (miR-134-5p, miR-136-3p, miR-142-3p, miR-143-3p, miR-145-3p, miR-146a-5p, miR-150-5p, miR-181d-5p, miR-199a-3p, miR-223-3p, miR-224-5p, miR-24-3p, miR-26a-5p, miR-28-5p, miR-29a-3p, miR-335-5p, miR-342-3p, miR-3605-3p, miR-3651,

miR-376c-3p, miR-3940-3p, miR-3960, miR-423-3p, miR-4286, miR-484, miR-487b-3p, miR-744-5p, miR-874-3p, miR-92b-3p) for further investigation, using the criteria of FDR < 0.1 and absolute $\log_2$ fold change > 1.0. 23 miRNAs were downregulated and 6 were upregulated [Supplementary Table 2]. Among these, miR-143-3p was the only miRNA with differential expression in both total plasma and the sEV-enriched fraction. Additionally, four miRNAs (miR-3960, miR-26a-5p, miR-142-3p, miR-423-3p) were included based solely on their regulation in the sEV-fraction (lipedema obese *vs.* obese comparison).

RT-qPCR cross-validation identifies robust plasma miRNA markers of lipedema and confirms lack of sEV differences

RT-qPCR cross-validations were performed to assess the robustness of the miRNA profiles using targeted analysis of selected miRNA candidates. First, NGS results were confirmed by re-analysis of the same RNA samples. Secondly, we recruited additional non-obese and lipedema participants, achieving a total group size of 16 non-obese controls and 12 lipedema patients for independent validation and final selection of a miRNA biomarker panel. In case of plasma sEVs, the RT-qPCR data did not identify any significant differences, thereby confirming the NGS results (data not shown). For total plasma samples, we compared NGS and RT-qPCR data by ROC analysis for each miRNA, focusing on the comparison of lipedema *vs.* non-obese control and lipedema obese *vs.* obese control and comparing the resulting AUC-values between both methods [Figure 4A]. Interestingly, we observed that NGS had underestimated effects for lipedema *vs.* BMI-matched control, and overestimated effects for lipedema obese *vs.* obese. However, five miRNAs with consistent differences between the groups could be identified: miR-223-3p, miR-224-5p, miR-3651, miR-484, miR-92b-3p [Figure 4b-f].

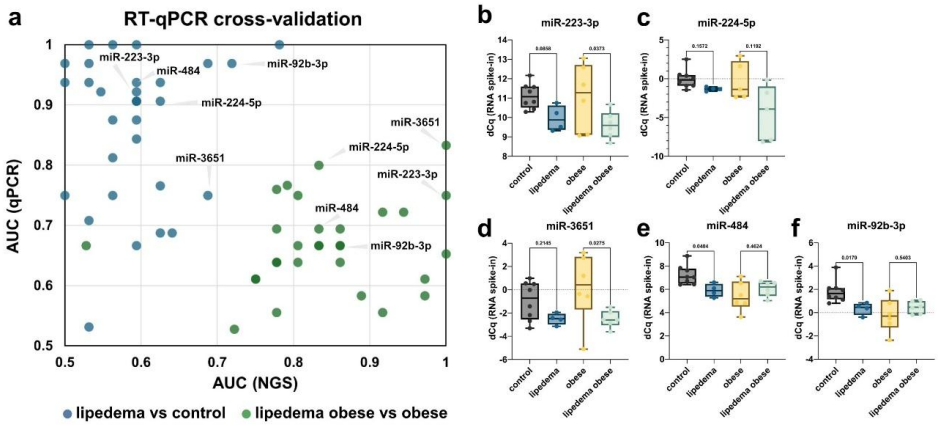

Figure 4. RT-qPCR confirmation of small RNA-sequencing results. (A) Comparison of RT-qPCR and NGS results for a panel of 29 miRNAs. AUC obtained from ROC analysis using either the NGS (x-axis) or RT-qPCR data (y-axis) are compared. Two comparisons are shown: lipedema *vs.* non obese controls (blue), and lipedema & obese *vs.* obese controls (green); (B-F) RT-qPCR data as delta Cq-values (dCq) relative to the spike-in control are shown for 5 miRNAs with consistent performance in the NGS and RT-qPCR analysis. Kruskal-Wallis Tests with Dunn´s multiple comparison test was used.

Multivariable modeling identifies miR-224-5p and miR-3651 as the optimal diagnostic combination

To assess the robustness of these results and investigate if the diagnostic performance could be improved by combining miRNAs into multivariable signatures, we first investigated whether the five miRNAs were regulated independently in lipedema. Pearson correlation analysis revealed that pairwise correlation coefficients ranged between 0.24 (miR-484 *vs.* miR-3651) and 0.94 (miR-92b-3p *vs.* miR-484), suggesting that combining miRNAs into classification models could improve the performance [Figure 5A]. Thus, multiple logistic regression analysis was performed stepwise, from 2 to 5 miRNAs, and resulting AUC-values were compared to the univariate models [Figure 5B]. The highest classification performance was achieved by combining miR-224-5p and miR-3651 (AUC 0.78), followed by the combination of all 5 miRNAs (AUC 0.77). ROC analysis for this pairwise combination resulted in a specificity of 75% at a set sensitivity of 92% [Figure 5C]. Finally, we applied the same prediction model (miR-224, miR-3651) to the obese and lipedema obese groups, which had not

been used for training the model, and observed a similar diagnostic performance [Figure 5D].

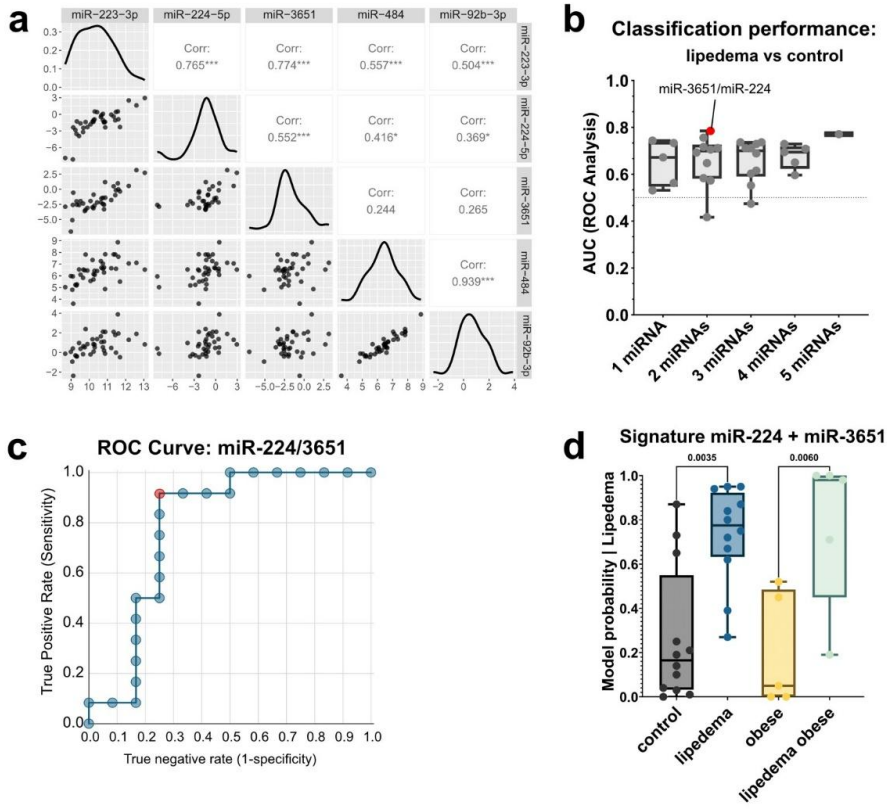

Figure 5. RT-qPCR data of all samples (*n* = 40). (A) Pearson correlation between each miRNA pair; (B) Classification performance expressed as area under the curve (AUC) from ROC analysis for univariable (1 miRNA) and multivariable miRNA signatures (2 to 5 miRNAs); (C) ROC curve illustrating lipedema diagnosis based on a model utilizing miR-224 and miR-3651 plasma levels;(D) lipedema diagnosis based on the miR-224 and miR-3651 prediction model.

Target prediction and Pathway analyses

For the five selected miRNAs regulated in lipedema (miR-223-3p, miR-224-5p, miR-3651, miR-484, miR-92b-3p), target prediction (Supplementary Table 3) and pathway analysis were performed and visualized as tree map plot, where the square size corresponds to the enrichment score within one biological process [Figure 6]. Ventricular septum morphogenesis was identified as most strongly enriched among the predicted targets followed by dsRNA transport, and plasma membrane raft assembly.

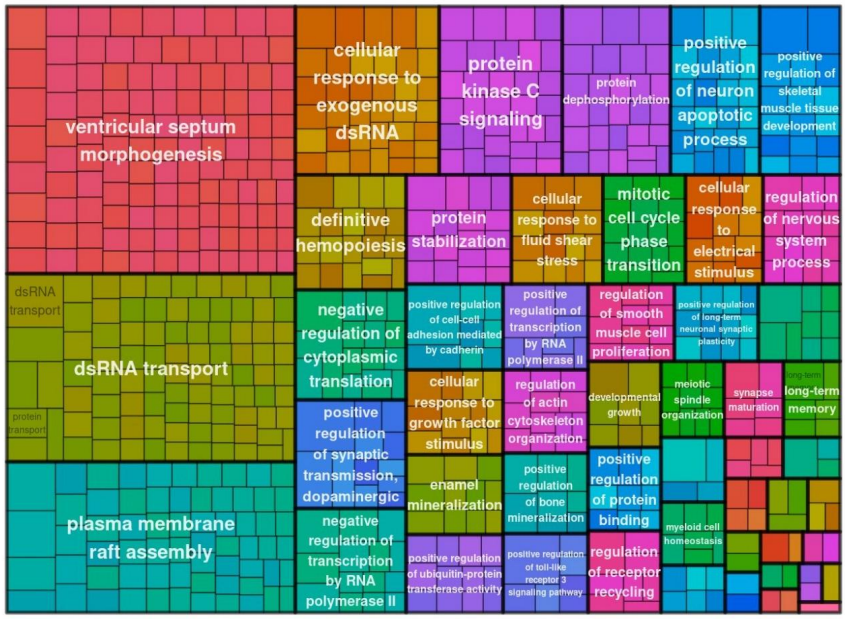

Figure 6. Biological processes affected by the targets of miRNAs differentially regulated in lipedema. Significantly enriched biological processes (BPs) are summarized based on similarity. Parent gene ontology (GO) terms and their child nodes are summarized in a tree map plot. The size of the squares corresponds to the enrichment score of each GO term.

DISCUSSION

We previously identified sEV miRNAs differentially secreted from early-stage lipedema SVF in comparison to non-obese controls[10]. This local miRNA signature was not reflected at the systemic level when investigating circulating plasma sEVs. This is likely due to minor contribution of adipose-derived sEVs to the total circulating EV pool. Since according to previous studies, platelets represent the major source of blood EVs, we have chosen PPP preparations as starting material[23]. Still, SVF-related surface markers were detected only at extremely low levels on plasma sEVs (data not shown) supporting the assumption that peripheral tissue-derived EVs represent only a small fraction of circulating EVs.

The overall pattern of differential miRNAs - as exemplified by the top 29 regulated candidates - represents the first description of circulating miRNA alterations associated with lipedema and highlights their potential role in lipedema pathophysiology. As disease associated biological pathways remain only partially understood, the findings of this study should be interpreted as exploratory and primarily hypothesis-generating

rather than evidence of causal mechanisms. These miRNAs are reportedly involved in vascular homeostasis, cardio-protection, lipid metabolism, stem cell functions, counteracting metabolic syndrome and type-2-diabetes/insulin resistance or modulation of inflammation and immune cells such as macrophage polarization. Interestingly, a substantial number of these miRNAs have also been reported in pain regulation, a central symptom of lipedema. Several downregulated miRNAs (e.g., miR-134-5p[28], miR-143-3p[29], miR-146a-5p[30], miR-223-3p[31]) have been reported to alleviate neuropathic and inflammatory pain in animal models. The observed downregulation, together with the reported chronic increase in systemic inflammatory and oxidative stress pathways[32] may reflect the chronic pain phenotype observed in most patients. Noteworthy, miR-29a-3p and miR24-3p, which were downregulated in the circulation of lipedema patients, were also significantly downregulated in SVF sEV of early-stage lipedema in our previous study[10]. Both miRNAs have been connected to inflammatory pain regulation[33,34]. This suggests a contribution of SVF-derived miRNAs to local pain and inflammation control.

Pathway analysis of the most consistently regulated miRNAs identified ventricular septum morphogenesis as one major process impacted by these molecules. While this finding should be interpreted cautiously, cardiovascular alterations such as significantly increased aortic stiffness based on transthoracic echocardiography have previously been reported[35]. Although lipedema patients have no severely increased cardiovascular risk or may even be protected from cardiovascular risk[36], cardiac abnormalities in the left ventricle (LV) and a dilated mitral annulus with impaired function have been reported[37].

Several miRNAs associated with endothelial dysfunction (miR-134-5p, miR-243-3p, miR-335-5p) and vascular damage (miR-142-3p, miR-92b-3p, miR-28-5p), cardiovascular disease (miR-134-5p, miR-145-3p, miR-335-5p), or suggested for classifying cardiovascular disease high-risk patients (miR-182-5p, miR-199a-5p, miR-193a-5p, and miR-155-5p, miR-223-3p miR-4286, miR-744-5p)[38] were downregulated in lipedema. Conversely, two miRNAs that have been associated with endothelial dysfunction, miR-484 und miR-3940-3p, were upregulated in lipedema in our study, and several miRNAs protective against vascular damage/ endothelial

dysfunction (miR-136-3p, miR-146a-5p, miR-1505p, miR-26a-5p) as well as cardioprotective (miR-224-5p, miR-24-3p, miR-28-5p, miR-376c-3p, miR-423-3p, miR-744-5p, miR-92b-3p) were downregulated. We therefore hypothesize that the combined dysregulation of vasculature-related miRNAs may reflect ongoing vascular imbalance in lipedema. This is also relevant, since chronic venous disease represents the most common (89%) comorbidity, affecting lipedema patients of all stages[39].

Several of the downregulated miRNAs (miR-143-3p miR-199a-3p, miR-29a-3p) have been reported to positively impact lymph angiogenesis. Previous studies have demonstrated lymphatic system dysregulation in lipedema pathophysiology, including impaired drainage, microvascular alterations and endothelial dysfunction[11].

Lipedema patients show an altered lipid profile and a lower prevalence of impaired glucose metabolism/insulin resistance, despite higher BMI, as compared to non-lipedema overweight/obesity[40]. In our study, small RNA sequencing identified 70 significantly downregulated and 10 significantly upregulated miRNAs in individuals with lipedema and increased BMI, compared to the matched (BMI > 30) controls. Among these downregulated miRNAs, some (e.g., miR-142, miR-143, miR-199a) are reportedly upregulated in obesity[41,42], some even downregulated (miR-146a, miR-150, miR-181d, miR-223-3p, miR-26a) in obesity. On the other hand, among the upregulated miRNAs in lipedema with BMI > 30, some are reportedly downregulated in obesity (miR-484, miR-874-3p, miR-92b-3p)[43-45]. Levels of miR-146-5p, miR-143, miR-423-3p have specifically been associated with risk of insulin resistance[42,46]. As many previous studies have already demonstrated, our findings on lipedema-specific miRNA signatures further support the concept that lipedema represents a biologically distinct adipose tissue condition that cannot be explained by BMI or obesity-associated mechanism.

For some of the regulated miRNAs (miR-143-3p, miR-181d, miRNA-223, miR-224-5p, miR-26a, miR26b, miR-335-5p, miR92b-3p) responsiveness to estradiol/ involvement in estrogen-signaling has been reported[47,48]. Lipedema appears and progresses most frequently in phases of hormonal changes and a link of the disease to estrogen signaling has been established[6,7,11]. Within the diseased tissue, lipedema reportedly involves an

altered estradiol metabolism/ estrogen receptor distribution, and in consequence local insulin resistance in adipocytes based on estrogen receptor alpha increased storage of sugar[7]. In our previous study on early-stage lipedema, we found an altered local estrogen metabolism together with upregulated ZNF423 (a driver of adipogenic commitment in preadipocytes) expression in adipose tissue and in derived pericytes and endothelial cells[11]. Interestingly, ZNF423 not only harbors estradiol binding sites but is also a predicted target of miR-224 (one of the two best-performing miRNAs in our study). Of note, in the plasma of transgender women, downregulation of sEV-contained miR-224 was detected after gender affirmative estradiol treatment, suggesting it as part of the estradiol post-transcriptional network leading to altered metabolism within adipose tissue or potentially at systemic level[49].

Although the study was executed with small cohorts, we applied stringent statistical analyses including correction for multiple testing. The observed sensitivity of 92% at 75% specificity for a model combining miR-224 and miR-3651 demonstrates promising clinical utility, which should be validated in larger independent cohorts in the future. The model performance was independent of lipedema stage, which is remarkable considering that within the lipedema obese cohort stages gradually more progressed than in the lipedema cohort. Most miRNAs were found downregulated in the disease, while in the obesity *vs.* non-obese group, they were rather upregulated. The miRNA signature identified in this study could be combined with other diagnostic criteria and blood-based biomarkers for lipedema diagnosis[18].

While these findings are exploratory - they demonstrate that plasma miRNA profiling can capture disease associated signals at a systemic level. Should the performance of the identified miRNA signature be validated, the ability to identify the disease in plasma samples would facilitate clinical trials and hence contribute to narrowing the treatment gap for this disease. Importantly, the availability of blood-based RT-qPCR testing would accelerate translation into clinical practice. The investigation of miRNA profiles in lipedema compared to non-disease individuals and to other conditions such as obesity might provide further understanding of its disease mechanisms, facilitating the development of targeted therapies.

DECLARATIONS

Acknowledgments

We thank Waltraud Tschulenk (Unit of Morphology, Vetmeduni, Austria) and Mukaddes Uezuelmez (LBI for Traumatology Austria) for their technical assistance with TEM and NTA of EV specimens, respectively.

Authors' contributions

Conceptualization: EP, MB, MS, MH, SW;

Methodology: EP, MB, MS, SM, VS, JOE, WH, SKS, MH, SW;

Software: MH;

Validation: MP, MH;

Formal analysis and investigation: EP, KM, MP, SM, VS, JOE, SKS, MH;

Data curation: EP, KM, MP, SM, VS, JOE, WH, SKS, MH;

Writing - original draft preparation: EP, KM, MB, MS, WH, MH, SW;

Writing - review and editing: EP, KM, MP, MB, MS, SM, VS, JOE, WH, SKS, MH, SW.

Availability of data and materials

All raw files from RNA analyses will be available in the gene expression omnibus (GEO) under accession number (GSE311356).

AI and AI-assisted tools Statement

During the preparation of this work, the authors used DeepL or ChatGPT 5.2 due to grammar and language enhancement. The authors reviewed and edited all AI-generated content carefully and take full responsibility for the final content of the manuscript.

Financial support and sponsorship

The study was supported by the Lipedema Foundation (Proof-of-concept award 2022; €100,000), which has been instrumental in funding research to define, diagnose, and develop treatments for lipedema. Their support has led to significant publications and advancements in the field (www.lipedema.org).

Conflicts of interest

All authors declared that there are no conflicts of interest.

Ethical approval and consent to participate

Ethical approval (Approval No. 1339/2021) from the local JKU ethical board, and all procedures were conducted in accordance with the Declaration of Helsinki. Written informed consent was obtained from all participants.

Consent for publication

Not applicable

Copyright

REFERENCES

1.Buso G, Depairon M, Tomson D, Raffoul W, Vettor R, Mazzolai L. Lipedema: A Call to Action! *Obesity (Silver Spring).* 2019;27(10):1567-76.[PMID: 31544340 PMCID: PMC6790573 DOI: 10.1002/oby.22597]

2.Amato ACM, Amato FCM, Amato JLS, Benitti DA. Lipedema prevalence and risk factors in Brazil. *J Vasc Bras*. 2022;21:e20210198.[PMID: 35677743 PMCID: PMC9136687 DOI: 10.1590/1677-5449.202101981]

3.Sandhofer M, Hofer V, Sandhofer M, Sonani M, Moosbauer W, Barsch M. High Volume Liposuction in Tumescence Anesthesia in Lipedema Patients: A Retrospective Analysis. *J Drugs Dermatol.* 2021;20(3):326-34.[PMID: 33683073 DOI: 10.36849/JDD.5828]

4.Sandhofer M, Hanke CW, Habbema L, Podda M, Rapprich S, Schmeller W, et al. Prevention of Progression of Lipedema With Liposuction Using Tumescent Local Anesthesia: Results of an International Consensus Conference. *Dermatol Surg.* 2020;46(2):220-8.[PMID: 31356433 DOI: 10.1097/DSS.0000000000002019]

5.van la Parra RFD, Deconinck C, Pirson G, Servaes M, Fosseprez P. Lipedema: What we don't know. *J Plast Reconstr Aesthet Surg.* 2023;84:302-12.[PMID: 37390539 DOI: 10.1016/j.bjps.2023.05.056]

6.Al-Ghadban S, Teeler ML, Bunnell BA. Estrogen as a Contributing Factor to the Development of Lipedema. *Physiology and Disorders of Adipose Tissue: IntechOpen;*

2021.[DOI: 10.5772/intechopen.96402]

7.Katzer K, Hill JL, McIver KB, Foster MT. Lipedema and the Potential Role of Estrogen in Excessive Adipose Tissue Accumulation. *Int J Mol Sci.* 2021;22(21).[PMID: 34769153 PMCID: PMC8583809 DOI: 10.3390/ijms222111720]

8.Kruppa P, Gohlke S, Lapinski K, Garcia-Carrizo F, Soultoukis GA, Infanger M, et al. Lipedema stage affects adipocyte hypertrophy, subcutaneous adipose tissue inflammation and interstitial fibrosis. *Front Immunol.* 2023;14:1223264.[PMID: 37575263 PMCID: PMC10417720 DOI: 10.3389/fimmu.2023.1223264]

9.Priglinger E, Wurzer C, Steffenhagen C, Maier J, Hofer V, Peterbauer A, et al. The adipose tissue-derived stromal vascular fraction cells from lipedema patients: Are they different? *Cytotherapy.* 2017;19(7):849-60.[PMID: 28454682 DOI: 10.1016/j.jcyt.2017.03.073]

10.Priglinger E, Strohmeier K, Weigl M, Lindner C, Auer D, Gimona M, et al. SVF-derived extracellular vesicles carry characteristic miRNAs in lipedema. *Sci Rep.* 2020;10(1):7211.[PMID: 32350368 PMCID: PMC7190633 DOI: 10.1038/s41598-020-64215-w]

11.Strohmeier K, Hofmann M, Jacak J, Narzt MS, Wahlmueller M, Mairhofer M, et al. Multi-Level Analysis of Adipose Tissue Reveals the Relevance of Perivascular Subpopulations and an Increased Endothelial Permeability in Early-Stage Lipedema. *Biomedicines.* 2022;10(5).[PMID: 35625899 PMCID: PMC9138324 DOI: 10.3390/biomedicines10051163]

12.Herbst KL, Kahn LA, Iker E, Ehrlich C, Wright T, McHutchison L, et al. Standard of care for lipedema in the United States. *Phlebology.* 2021;36(10):779-96.[PMID: 34049453 PMCID: PMC8652358 DOI: 10.1177/02683555211015887]

13.Crescenzi R, Marton A, Donahue PMC, Mahany HB, Lants SK, Wang P, et al. Tissue Sodium Content is Elevated in the Skin and Subcutaneous Adipose Tissue in Women with Lipedema. *Obesity (Silver Spring).* 2018;26(2):310-7.[PMID: 29280322 PMCID: PMC5783748 DOI: 10.1002/oby.22090]

14.Wolf S, Deuel JW, Hollmen M, Felmerer G, Kim BS, Vasella M, et al. A Distinct Cytokine Profile and Stromal Vascular Fraction Metabolic Status without Significant Changes in the Lipid Composition Characterizes Lipedema. *Int J Mol Sci.* 2021;22(7).[PMID: 33805070 PMCID: PMC8036495 DOI: 10.3390/ijms22073313]

15.Hansmeier NR, Buschlen IS, Behncke RY, Ulferts S, Bisoendial R, Hagerling R. 3D

Visualization of Human Blood Vascular Networks Using Single-Domain Antibodies Directed against Endothelial Cell-Selective Adhesion Molecule (ESAM). *Int J Mol Sci.* 2022;23(8).[PMID: 35457187 PMCID: PMC9028812 DOI: 10.3390/ijms23084369]

16.Kempa S, Buechler C, Foh B, Felthaus O, Prantl L, Gunther UL, et al. Serum Metabolomic Profiling of Patients with Lipedema. *Int J Mol Sci*. 2023;24(24).[PMID: 38139266 PMCID: PMC10743543 DOI: 10.3390/ijms242417437]

17.Al-Wardat M, Alwardat N, Lou De Santis G, Zomparelli S, Gualtieri P, Bigioni G, et al. The association between serum vitamin D and mood disorders in a cohort of lipedema patients. *Horm Mol Biol Clin Investig.* 2021;42(4):351-5.[PMID: 34323062 DOI: 10.1515/hmbci-2021-0027]

18.Ma W, Gil HJ, Escobedo N, Benito-Martin A, Ximenez-Embun P, Munoz J, et al. Platelet factor 4 is a biomarker for lymphatic-promoted disorders. *JCI Insight.* 2020;5(13).[PMID: 32525843 PMCID: PMC7406300 DOI: 10.1172/jci.insight.135109]

19.O'Brien J, Hayder H, Zayed Y, Peng C. Overview of MicroRNA Biogenesis, Mechanisms of Actions, and Circulation. *Front Endocrinol (Lausanne).* 2018;9:402.[PMID: 30123182 PMCID: PMC6085463 DOI: 10.3389/fendo.2018.00402]

20.Arroyo JD, Chevillet JR, Kroh EM, Ruf IK, Pritchard CC, Gibson DF, et al. Argonaute2 complexes carry a population of circulating microRNAs independent of vesicles in human plasma. *Proc Natl Acad Sci U S A.* 2011;108(12):5003-8.[PMID: 21383194 PMCID: PMC3064324 DOI: 10.1073/pnas.1019055108]

21.Vanhaverbeke M, Attard R, Bartekova M, Ben-Aicha S, Brandenburger T, de Gonzalo-Calvo D, et al. Peripheral blood RNA biomarkers for cardiovascular disease from bench to bedside: a position paper from the EU-CardioRNA COST action CA17129. *Cardiovasc Res.* 2022;118(16):3183-97.[PMID: 34648023 PMCID: PMC9799060 DOI: 10.1093/cvr/cvab327]

22.Landrier JF, Derghal A, Mounien L. MicroRNAs in Obesity and Related Metabolic Disorders. *Cells.* 2019;8(8).[PMID: 31404962 PMCID: PMC6721826 DOI: 10.3390/cells8080859]

23.Mussbacher M, Krammer TL, Heber S, Schrottmaier WC, Zeibig S, Holthoff HP, et al. Impact of Anticoagulation and Sample Processing on the Quantification of Human Blood-Derived microRNA Signatures. *Cells.* 2020;9(8).[PMID: 32824700 PMCID:

PMC7464075 DOI: 10.3390/cells9081915]

24.Oesterreicher J, Pultar M, Schneider J, Muehleder S, Zipperle J, Grillari J, et al. Fluorescence-Based Nanoparticle Tracking Analysis and Flow Cytometry for Characterization of Endothelial Extracellular Vesicle Release. *Int J Mol Sci,* 2020. 21(23).[PMID: 33291792 PMCID: PMC7731108 DOI: 10.3390/ijms21239278]

25.Chaves-Solano N, Kau-Strebinger S, Oesterreicher J, Pultar M, Holnthoner W, Grillari J, et al. Distinct miRNA profiles in human amniotic tissue and its vesicular and non-vesicular secretome. *Front Cell Dev Biol,* 2025. 13: p. 1692501.[PMID: 41234360 PMCID: PMC12605191 DOI: 10.3389/fcell.2025.1692501]

26.Khamina K, Diendorfer AB, Skalicky S, Weigl M, Pultar M, Krammer TL, et al. A MicroRNA Next-Generation-Sequencing Discovery Assay (miND) for Genome-Scale Analysis and Absolute Quantitation of Circulating MicroRNA Biomarkers. *Int J Mol Sci.* 2022;23(3).[PMID: 35163149 PMCID: PMC8835905 DOI: 10.3390/ijms23031226]

27.Diendorfer A, Khamina K, Pultar M, Hackl M. miND (miRNA NGS Discovery pipeline): a small RNA-seq analysis pipeline and report generator for microRNA biomarker discovery studies. *F1000Research.* 2022;11:233.[PMID: 42147075 PMCID: PMC13173284 DOI: 10.12688/f1000research.94159.2]

28.Ji LJ, Su J, Xu AL, Pang B, Huang QM. MiR-134-5p attenuates neuropathic pain progression through targeting Twist1. *J Cell Biochem.* 2019;120(2):1694-701.[PMID: 30187947 DOI: 10.1002/jcb.27486]

29.Tan PH, Pao YY, Cheng JK, Hung KC, Liu CC. MicroRNA-based therapy in pain medicine: Current progress and future prospects. *Acta Anaesthesiol Taiwan.* 2013;51(4):171-6.[PMID: 24529673 DOI: 10.1016/j.aat.2013.11.001]

30.Lu Y, Cao DL, Jiang BC, Yang T, Gao YJ. MicroRNA-146a-5p attenuates neuropathic pain via suppressing TRAF6 signaling in the spinal cord. *Brain Behav Immun.* 2015;49:119-29.[PMID: 25957028 DOI: 10.1016/j.bbi.2015.04.018]

31.Huang B, Guo S, Zhang Y, Lin P, Lin C, Chen M, et al. MiR-223-3p alleviates trigeminal neuropathic pain in the male mouse by targeting MKNK2 and MAPK/ERK signaling. *Brain Behav.* 2022;12(7):e2634.[PMID: 35608154 PMCID: PMC9304854 DOI: 10.1002/brb3.2634]

32.Nankam PAN, Cornely M, Kloting N, Bluher M. Is subcutaneous adipose tissue expansion in people living with lipedema healthier and reflected by circulating

parameters? *Front Endocrinol (Lausanne).* 2022;13:1000094.[PMID: 36387874 PMCID: PMC9659629 DOI: 10.3389/fendo.2022.1000094]

33.Guo R, Fang Y, Zhang Y, Liu L, Li N, Wu J et al. SHED-derived exosomes attenuate trigeminal neuralgia after CCI of the infraorbital nerve in mice via the miR-24-3p/IL-1R1/p-p38 MAPK pathway. *J Nanobiotechnology.* 2023;21(1):458.[PMID: 38031158 PMCID: PMC10685568 DOI: 10.1186/s12951-023-02221-6]

34.Liu CC, Hung KC, Li YY, Yi-Kung Huang E, Chu CC, Chow LH, et al. The concerted actions of microRNA-29a and interferon-beta modulate complete Freund's adjuvant-induced inflammatory pain by regulating the expression of type 1 interferon receptor, interferon-stimulated gene 15, and p-extracellular signal-regulated kinase. *BJA Open.* 2025;13:100376.[PMID: 39980495 PMCID: PMC11840201 DOI: 10.1016/j.bjao.2024.100376]

35.Szolnoky G, Nemes A, Gavaller H, Forster T, Kemeny L. Lipedema is associated with increased aortic stiffness. *Lymphology.* 2012;45(2):71-9.[PMID: 23057152]

36.Pinnick KE, Nicholson G, Manolopoulos KN, McQuaid SE, Valet P, Frayn KN, et al. Distinct developmental profile of lower-body adipose tissue defines resistance against obesity-associated metabolic complications. *Diabetes.* 2014;63(11):3785-97.[PMID: 24947352 DOI: 10.2337/db14-0385]

37.Nemes A, Kormanyos A, Domsik P, Kalapos A, Gyenes N, Kemeny L, et al. Are increased left ventricular strains compensatory effects in lipedema? Detailed analysis from the three-dimensional speckle-tracking echocardiographic MAGYAR-Path Study. *J Clin Ultrasound.* 2020;48(8):470-5.[PMID: 32394509 DOI: 10.1002/jcu.22855]

38.Elmoselhi AB, Seif Allah M, Bouzid A, Ibrahim Z, Venkatachalam T, Siddiqui R, et al. Circulating microRNAs as potential biomarkers of early vascular damage in vitamin D deficiency, obese, and diabetic patients. *PLoS One.* 2023;18(3):e0283608.[PMID: 36952563 PMCID: PMC10035929 DOI: 10.1371/journal.pone.0283608]

39.Luta X, Buso G, Porceddu E, Psychogyiou R, Keller S, Mazzolai L. Clinical characteristics, comorbidities, and correlation with advanced lipedema stages: A retrospective study from a Swiss referral centre. *PLoS One.* 2025;20(3):e0319099.[PMID: 40111978 PMCID: PMC11925301 DOI: 10.1371/journal.pone.0319099]

40.Jeziorek M, Wuczynski M, Sowicz M, Adaszynska A, Szuba A, Chachaj A.

Metabolic Alterations in Women with Lipedema Compared to Women with Lifestyle-Induced Overweight/Obesity. *Biomedicines.* 2025;13(4).[PMID: 40299449 PMCID: PMC12024828 DOI: 10.3390/biomedicines13040867]

41.Matveev GA, Khromova NV, Zasypkin GG, Kononova YA, Vasilyeva EY, Babenko AY, et al. Tissue and Circulating MicroRNAs 378 and 142 as Biomarkers of Obesity and Its Treatment Response. *Int J Mol Sci.* 2023;24(17).[PMID: 37686231 PMCID: PMC10487855 DOI: 10.3390/ijms241713426]

42.Xihua L, Shengjie T, Weiwei G, Matro E, Tingting T, Lin L, et al. Circulating miR-143-3p inhibition protects against insulin resistance in Metabolic Syndrome via targeting of the insulin-like growth factor 2 receptor. *Transl Res.* 2019;205:33-43.[PMID: 30392876 DOI: 10.1016/j.trsl.2018.09.006]

43.Abu-Farha M, Cherian P, Al-Khairi I, Nizam R, Alkandari A, Arefanian H, et al. Reduced miR-181d level in obesity and its role in lipid metabolism via regulation of ANGPTL3. *Sci Rep.* 2019;9(1):11866.[PMID: 31413305 PMCID: PMC6694160 DOI: 10.1038/s41598-019-48371-2]

44.Fu X, Dong B, Tian Y, Lefebvre P, Meng Z, Wang X, et al. MicroRNA-26a regulates insulin sensitivity and metabolism of glucose and lipids. *J Clin Invest.* 2015;125(6):2497-509.[PMID: 25961460 PMCID: PMC4497741 DOI: 10.1172/JCI75438]

45.Zmyslowska A, Smyczynska U, Stanczak M, Jeziorny K, Szadkowska A, Fendler W, et al. Association of circulating miRNAS in patients with Alstrom and Bardet-Biedl syndromes with clinical course parameters. *Front Endocrinol (Lausanne).* 2022;13:1057056.[PMID: 36506055 PMCID: PMC9732093 DOI: 10.3389/fendo.2022.1057056]

46.Santos D, Porter-Gill P, Goode G, Delhey L, Sorensen AE, Rose S, et al. Circulating microRNA levels differ in the early stages of insulin resistance in prepubertal children with obesity. *Life Sci.* 2023;312:121246.[PMID: 36455651 PMCID: PMC10375861 DOI: 10.1016/j.lfs.2022.121246]

47.Pan Q, Ma J, Guo K. miR-223 Enhances the Neuroprotection of Estradiol Against Oxidative Stress Injury by Inhibiting the FOXO3/TXNIP Axis. *Neurochem Res.* 2022;47(7):1865-77.[PMID: 34843004 DOI: 10.1007/s11064-021-03490-z]

48.Zhang S, Liu Y, Wang M, Ponikwicka-Tyszko D, Ma W, Krentowska A, et al. Role and mechanism of miR-335-5p in the pathogenesis and treatment of polycystic ovary

syndrome. *Transl Res.* 2023;252:64-78.[PMID: 35931409 DOI: 10.1016/j.trsl.2022.07.007]

49.Florijn BW, Duijs J, Klaver M, Kuipers EN, Kooijman S, Prins J, et al. Estradiol-driven metabolism in transwomen associates with reduced circulating extracellular vesicle microRNA-224/452. *Eur J Endocrinol.* 2021;185(4):539-52.[PMID: 34342596 PMCID: PMC8436186 DOI: 10.1530/EJE-21-0267]